Langmuir

Article

pubs.acs.org/Langmuir

Macroscopic Theory for Capillary-Pressure Hysteresis

Bhagya Athukorallage,*[,†] Eugenio Aulisa,[†] Ram Iyer,[†] and Larry Zhang[‡]

[†]Department of Mathematics and Statistics, Texas Tech University, Lubbock, Texas 79409, United States

[‡]Harvard Westlake, Coldwater Canyon Avenue, Studio City, California 91604, United States

ABSTRACT: In this article, we present a theory of macroscopic contact angle hysteresis by considering the minimization of the Helmholtz free energy of a solid−liquid−gas system over a convex set, subject to a constant volume constraint. The liquid and solid surfaces in contact are assumed to adhere weakly to each other, causing the interfacial energy to be set-valued. A simple calculus of variations argument for the minimization of the Helmholtz energy leads to the Young−Laplace equation for the drop surface in contact with the gas and a variational inequality that yields contact angle hysteresis for advancing/receding flow. We also show that the Young−Laplace equation with a Dirichlet boundary condition together with the variational inequality yields a basic hysteresis operator that describes the relationship between capillary pressure and volume. We validate the theory using results from the experiment for a sessile macroscopic drop. Although the capillary effect is a complex phenomenon even for a droplet as various points along the contact line might be pinned, the capillary pressure and volume of the drop are scalar variables that encapsulate the global quasistatic energy information for the entire droplet. Studying the capillary pressure versus volume relationship greatly simplifies the understanding and modeling of the phenomenon just as scalar magnetic hysteresis graphs greatly aided the modeling of devices with magnetic materials.

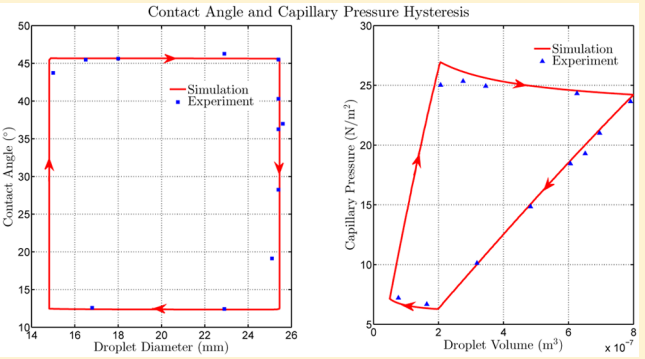

1. INTRODUCTION

The study of capillary interfaces is an important research area due to its prominent roles in soil science, plant biology, and surface physics (self-cleaning surfaces), among others. Because of interfacial molecular interactions, the boundary of a capillary surface behaves in certain ways based on the chemical properties of the liquid, substrate, and medium surrounding the liquid and the substrate's smoothness and uniformity.[1] The combination of all of these factors provides the basis for the definition of the property of a liquid−surface interface known as wetting, which describes the degree to which a liquid spreads on a substrate. It has been known since the work of Sulman and Picard[2] that there is a difference in the contact angle at the solid−liquid−gas contact line between rising drops and falling drops, a phenomenon they termed contact angle hysteresis. The amount of hysteresis depends on the chemical compositions of the solid and the liquid and the physical roughness of the surface.[3] Several researchers have shown through very careful experiments that even for solids with surface height variation in the nanometer range and drop sizes that are 2 or 3 orders of magnitude larger, there is still significant contact angle hysteresis.[4−7] These results show that the solid−liquid chemistry is the primary reason for the contact angle hysteresis. The same experiments have also shown that increases in surface roughness change the amount of contact angle hysteresis but in a consistent manner, that is, a given solid sample and a given liquid will yield a consistent measurement of advancing and receding angles provided the drop sizes are 2 or 3 orders of magnitude larger than the height variations of the solid.[3,8]

Several different solid−liquid−gas configurations may be studied such as a sessile drop, a confined drop inside a capillary tube, or a drop between two solid plates. In this article, we present a theory that is applicable to drops in all of the above configurations, when volume is changed in a quasi-static manner at constant temperature. However, in this article, the theory is validated for sessile drops only. The theory is macroscopic in nature; that is, it is applicable to drops with a length of contact between liquid and solid that is 2 or 3 orders of magnitude larger than height variations of the solid. This is because liquid films on a solid substrate with a length of contact comparable to height variations of the solid deviate from the drop shape predicted by the Young−Laplace equation as intermolecular forces between solid and liquid need to be accounted for.[3,9,10]

At constant temperature and volume, the wetting of the solid surface is a consequence of the droplet−solid surface−gas system spontaneously changing so as to decrease the Helmholtz free energy of the system. The Helmholtz energy of the system is the sum of the interfacial energies of solid−gas, solid−liquid, gas−liquid, and potential energy density due to gravitation. The interfacial energies per unit area are given by γ_{SG} between the

Received: November 18, 2014
Revised: January 29, 2015

DOI: 10.1021/la504495c
Langmuir XXXX, XXX, XXX−XXX

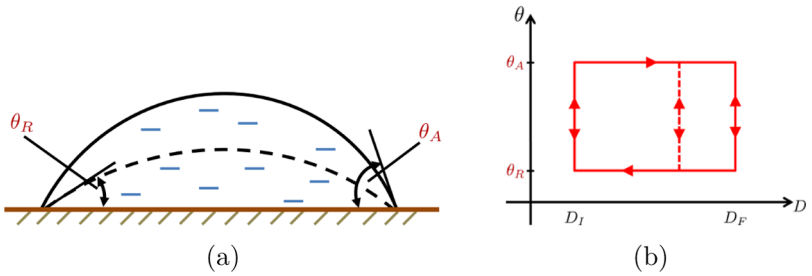

Figure 1. (a) Contact angle hysteresis effect: advancing and receding contact angles of a liquid drop. (b) Plot of the contact angle θ versus contact diameter D for a drop on a solid surface.

substrate and gas, γ_{SL} between the substrate and liquid, and γ_{LG} between the liquid and gas.

The starting point of our theory is the assumption that quantity γ_{SL} is set-valued. We explain the rationale behind this assumption next. As experiments have pointed out that the primary reason for contact angle hysteresis is the chemistry between the solid and liquid,[4−7] the practice of assigning only a single value for the interfacial energy γ_{SL} was questioned by Penn and Miller.[5] Recently, Snoeijer and Andreotti[10] have shown through a theoretical analysis at the microscopic level of a liquid drop on a smooth surface with no surface roughness and with no chemical impurities that the macroscopic (or apparent) contact angle must be set-valued. Extrand[11] started with the assumption that the advancing and receding contact angles are known and concluded that the interfacial energy of the solid−liquid must be set-valued if the angles are different. In our theory, we start from the assumption of set-valued interfacial energy for the solid−liquid interface and show how the contact angle hysteresis and flow rules follow as a consequence of the second law of thermodynamics. To be precise, we show that for a given volume and temperature the minimization of the Helmholtz energy over the closed, convex set where γ_{SL} takes values leads to a variational inequality that immediately yields the flow rules of contact angle hysteresis. Furthermore, we present evidence from experiment on macroscopic sessile drops that the relation between the capillary pressure and volume of the liquid shows hysteresis. Because of this hysteresis relation, net work must be done by an external agent while changing the volume of the droplet through a cycle.

1.1. Contact Angle Hysteresis. In this section, we briefly present the phenomenon of macroscopic contact angle hysteresis. In section 2, we present a variational theory that predicts the phenomenon of contact angle hysteresis when there is some adhesion between solid and liquid molecules. In section 3, we describe precisely how the contact angles are measured in experiments.

Consider a liquid droplet on a solid surface with a contact angle of θ (refer to Figure 1). Experiments (section 3 of this article) show that if the liquid is carefully added to the droplet via a syringe then the volume and contact angle of the droplet increases without changing its initial contact area. Further increases in its volume results in an increase in the contact area with the contact angle fixed at θ_A (refer to Figure 1a). Similarly, if the liquid is removed from a droplet, then the volume and contact angle of the droplet decrease but retain the same contact area. Continuing this process results in a recession of the contact area at a contact angle of θ_R (refer to Figure 1b).[1,12] The limiting values, θ_A and θ_R, are referred to as advancing and receding angles. For a symmetric droplet, one can obtain a hysteresis diagram for the contact angle θ versus droplet diameter D as depicted in Figure 1b. For a general droplet, the contact angle may take on different values at different points along the contact line; however, the contact line is pinned at a point unless the contact angle is equal to either the advancing or receding angle.

1.2. Energy Losses Due to Hysteresis. A liquid advances or recedes on the solid substrate once the attraction force between solid and liquid molecules is overcome at the contact line. This process requires an expenditure of energy by the external agent causing the liquid to advance or recede. Therefore, if one cycle of advancement and recession is completed, then there is a positive net work done by the external agent. A study of the relation between the contact angle and the wetted area reveals a certain structure and pattern which justifies the use of the term "hysteresis" in the same operator theoretical sense found in the literature.[13−16]

In this article, we attempt to fill a gap in the current understanding of the capillary phenomenon by investigating the relationship between the capillary pressure and volume. The phenomenology of hysteresis in the capillary effect is due to weak forces between the solid and liquid molecules that are in contact. Because of this effect, multiple droplet shapes for the same fixed volume are possible although these shapes have different capillary pressure and as a result have different Helmholtz energies. We show in this article that the capillary pressure versus volume graph shows hysteresis. Although the capillary effect is a complex phenomenon even for a droplet as various points along the contact line might be pinned (unable to move instantaneously), the capillary pressure and volume of the drop are scalar variables that encapsulate the global quasistatic energy information for the entire droplet. This greatly simplifies the modeling of the phenomenon, especially in computational fluid dynamics models.

1.3. Related Work. An algorithm for the simulation of drops on planar surfaces both flat and inclined is presented in Santos et al.[17,18] For inclined surfaces, the authors directly minimize the Helmholtz energy functional subject to a volume constraint and rules for the advancement and recession of the contact line. A similar methodology is also found in Janardan et al.[19] In our work, we show that such rules directly follow from a variational inequality that results from the minimization of the Helmholtz energy over a convex set (section 2.1).

Chen et al.[20] consider the deformation of a liquid bridge formed between two horizontal solid surfaces. Both surfaces are nonideal, and contact angle hysteresis is observed. The authors observe that the liquid bridge possesses two different equilibrium profiles with the same distance of separation of the solid surfaces. On the basis of the adhesion force and the distance of separation of the two horizontal plates, the energy

DOI: 10.1021/la504495c
Langmuir XXXX, XXX, XXX−XXX

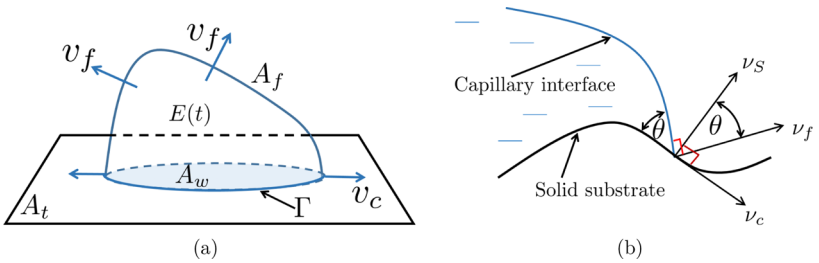

Figure 2. (a) Schematic representation of a liquid drop on a solid substrate. The shape of the drop at time t is $E(t)$. (b) Geometric definition of the contact angle for a 3-D droplet on a solid substrate: ν_S is the normal to the solid substrate at the contact line, and ν_f is the normal to the droplet surface at the contact line. The angle between ν_S and ν_f is the contact angle.

dissipation during a quasi-static stretching and compression cycle is calculated using the area enclosed by the adhesion force−surface separation curve. As the volume remains constant, the loss is entirely due to line motion. The rules for the line motion follow from our results in section 2.1. The energy loss may be accommodated by a Rayleigh-type dissipation function described in section 2.2.

Alberti et al.[21] proposed a model for the quasi-static evolution of a drop and contact angle hysteresis. The work presented here differs from their work in several respects. First, they consider kinetic friction that opposes line motion as the cause of contact angle hysteresis, whereas we consider Coulomb static friction caused by weak forces between solid and liquid molecules to be the cause of contact angle hysteresis. The loss functional in Alberti et al.[21] is directly proportional to the magnitude of the velocity of the line motion, which implies that for a quasistatic change in volume there is no energy lost. In our model, the energy loss is directly related to rate-independent hysteresis between the capillary pressure (p) and volume (ω). When the plot of pressure versus volume is a loop in the $p - \omega$ plane, the energy lost for quasistatic variation in volume is given by the area of the loop. Second, in Alberti et al.,[21] rules for contact angle hysteresis are postulated, whereas we show that such rules directly follow from a variational inequality that results from a minimization of the Helmholtz energy over a convex set. Third, although the complex contact angle hysteresis phenomenon on each point of the contact line causes energy loss, we show that the relationship between scalar variables p and ω contains the energy loss information, and we may use this relationship in a predictive model.

Finally, we address the theories of contact angle hysteresis that start with the assumption that surface roughness is the primary cause of contact angle hysteresis. Johnson et al.[22] assume a single contact angle at the solid−liquid−gas contact line and study the metastable states caused by a periodic surface roughness function. As mentioned earlier, the hypothesis of a unique contact angle is not supported by experimental evidence that shows that even with nanometer-sized variations in surface and macroscopic droplets, contact angle hysteresis is observed.[5−7] In a series of articles,[23−26] another theory is developed where a rough surface is homogenized, leading to a single homogenized contact angle, and contact angle hysteresis is introduced via the assumption that chemical impurities resist the motion of the contact line. On the other hand, a theoretical microscopic analysis of a solid surface that is completely smooth and devoid of chemical impurities on the microscopic level shows that contact angle hysteresis is still possible due to weak forces between solid and liquid molecules at the interface.[10] An important point about the presence of surface roughness is that although the contact angle hysteresis is modified due to the roughness,[4−6] the experimental results are reproducible. In our work, the starting point is the assumption that the interfacial energy γ_{SL} is set-valued; the cause could be a combination of chemistry and surface roughness, and this possibility does not alter the validity of the assumption and the conclusions of our theory.

2. LIQUID DROP ON A SOLID SURFACE

2.1. Necessary Condition for a Minimizer of the Energy Functional over a Convex Set. We perform a quasistatic analysis of a liquid drop on a solid plate subject to a time-varying volume constraint as described in ref 21. Let $E(t)$ denote a regular region in $\mathbb{R}^3$ occupied by the liquid drop at time t, and let $|E(t)|$ denote the measure of $E(t)$ as the volume of the drop (Figure 2a). The drop encounters three different phases: solid−liquid (SL), solid−gas (SG), and liquid−gas (LG). Each interface between phases is associated with an interfacial energy, and we denote these using γ_{SL}, γ_{SG}, and γ_{LG}. Let A_t, A_f, and A_w be the total area of the solid substrate, area of the free surface, and area of contact region of the solid and the droplet, respectively. The common boundary of A_f and A_w is Γ. The velocities of the free surface and the contact line are v_f and v_c, in the corresponding outward normal directions. Let $\omega(t)$ be the volume of the droplet at a given time t.

We consider an isothermal condition and formulate the Helmholtz free energy of the system, $\mathcal{E}$, which contains the surface energy of the meniscus, surface energies of the solid−liquid and solid−gas interfaces, and potential energy due to gravity.

$$\mathcal{E} = \gamma_{LG}A_f + \gamma_{SG}(A_t - A_w) + \gamma_{SL}A_w + \int_{E(t)} \psi(x, t)\, dV$$
$$= \gamma_{LG}A_f + A_w(\gamma_{SL} - \gamma_{SG}) + A_t\gamma_{SG} + \int_{E(t)} \psi(x, t)\, dV \quad (1)$$

Here, $\psi(x, t)$ is the potential energy density due to gravity, and dV denotes the volume element of the drop. The very formulation of the free energy above implies a macroscopic viewpoint where the size of the drop is much larger than the surface asperities so that bulk energies dominate. On the microscopic level, weak forces between solid and liquid modify the energy $\mathcal{E}$. This modification may be accounted for in macroscopic theory by assuming γ_{SL} to take values in an interval, that is, $\gamma_{SL} \in [\gamma_{SL_{min}}, \gamma_{SL_{max}}]$. The physical cause of the set-valued γ_{SL} may be purely chemistry between the solid and the liquid[5,10] or a combination of chemistry and surface roughness.

DOI: 10.1021/la504495c
Langmuir XXXX, XXX, XXX−XXX

Following Alberti and DeSimone,[21] we define $\cos\theta_Y := (\gamma_{SG} - \gamma_{SL})/\gamma_{SG}$, and eq 1 may be expressed as

$$\mathcal{E} = \gamma_{LG}\left(A_f - A_w\cos\theta_Y + A_t\frac{\gamma_{SG}}{\gamma_{LG}} + \frac{1}{\gamma_{LG}}\int_{E(t)}\psi(x,t)\,dV\right) \tag{2}$$

Suppose that the volume constraint $|E(t)| = \omega(t)$ is prescribed $\forall t \in [t_0, t_1]$. Note that for an isothermal system, changes in the Helmholtz free energy must be negative.[27] For a fixed t, the virtual variation of $\mathcal{E}$ with respect to $E(t)$, subject to the constraint $|E(t)| = \omega(t)$, yields[28]

$$\delta\mathcal{E} + \frac{p(t)}{\gamma_{LG}}\delta|E(t)| \le 0 \tag{3}$$

over the set of admissible variations and $\cos\theta_Y \in [\cos\theta_A, \cos\theta_R]$, where θ_A and θ_R are the advancing and receding contact angles. We have the relations $\cos\theta_A := (\gamma_{SG} - \gamma_{SL_{max}})/\gamma_{LG}$ and $\cos\theta_R := (\gamma_{SG} - \gamma_{SL_{min}})/\gamma_{LG}$. In eq 3, $p(t)$ is the associated Lagrange multiplier for the volume constraint. Inequality 3 reduces to

$$\int_{A_f(t)} -2Hv_f\,dS_f + \int_{\Gamma(t)}\cos\theta\, v_c dl - \int_{\Gamma(t)}\cos\theta_Y\,\mathbf{v}\cdot\nu\,dl + \frac{1}{\gamma_{LG}}\int_{\partial E(t)}\psi(x,t)\mathbf{v}\cdot\nu\,dS + \frac{1}{\gamma_{LG}}\int_{A_f(t)}p(t)v_f\,dS_f \le 0 \tag{4}$$

$\forall v_f$ and $\cos\theta_Y \in [\cos\theta_A, \cos\theta_R]$. Here, $\mathbf{v}$ is the velocity of a moving boundary, and ν is the outward-pointing normal vector of the boundary that corresponds to $\mathbf{v}$. H and θ denote the mean curvature of the free surface and the contact angle. Simplifying and rearranging the terms in eq 4 yield

$$\gamma_{LG}\left(\int_{A_f(t)}\left(-2H + \frac{\psi(x,t) + p(t)}{\gamma_{LG}}\right)v_f\,dS_f + \int_{\Gamma(t)}(\cos\theta - \cos\theta_Y)v_c\,dl\right) \le 0 \tag{5}$$

As v_f and v_c are independent variations, we may set $v_c = 0$, and we get

$$-2H + \frac{\psi(x,t) + p(t)}{\gamma_{LG}} = 0\ \forall\ v_f \in A_f \tag{6}$$

Next, we consider the variational inequality obtained by setting $v_f = 0$

$$(\cos\theta - \cos\theta_Y)v_c \le 0 \tag{7}$$

that yields from the second integral in eq 5 for $\cos\theta_Y \in [\cos\theta_A, \cos\theta_R]$. Note that the contact line velocity, v_c, is related to θ. For a particular θ value, v_c is determined by this variational inequality.

(i) If $\cos\theta \in (\cos\theta_A, \cos\theta_R)$, then $\forall\theta_Y$, $(\cos\theta - \cos\theta_Y)$ may be greater than, or equal to, or less than zero. Hence, by inequality 7, we may state that $v_c = 0$.
(ii) If $\cos\theta = \cos\theta_A$, then $\forall\theta_Y$, $(\cos\theta - \cos\theta_Y) \le 0$. Thus, by inequality 7, we may state that $v_c \ge 0$.
(iii) If $\cos\theta = \cos\theta_R$, then $\forall\theta_Y$, $(\cos\theta - \cos\theta_Y) \ge 0$. Hence, by inequality 7, we may state that $v_c \le 0$.

2.1.1. Remarks. For a prescribed volume $\omega(0)$ at time $t = 0$, eq 6 and inequality 7 may be solved together with a Dirichlet boundary condition that specifies that the liquid surface is attached to the solid along the contact line to find an equilibrium configuration for the drop. From this initial configuration, one may then solve for the volume at each successive instant of time. Note that one cannot specify both a Dirichlet boundary condition and a Neumann boundary condition for the contact angles at the contact line. This is because eq 6 is a second-order PDE. The Helmholtz energy $\mathcal{E}$ includes only an elastic energy term for the liquid surface in contact with gas in eq 2. If $\mathcal{E}$ is modified by adding a bending energy term of the form[29]

$$\text{bending energy} = \int_{A_f(t)}\frac{k_c}{2}((2H - c_0)^2 - K)\,dS_f \tag{8}$$

where k_c is the bending rigidity and c_0 is the spontaneous curvature, then the following equation results from inequality 3 in addition to variational inequality 7:

$$k_c(2H + c_0)(2H^2 - 2K - c_0H) + 2k_c\Delta H - 2H + \frac{\psi(x,t) + p(t)}{\gamma_{LG}} = 0 \tag{9}$$

The derivation of the first term may be found in Zhong-can and Helfrich.[29] The above equation is a fourth-order PDE and is a generalization of the Young−Laplace equation to the case where the liquid surface has bending energy in addition to the elastic stretching energy. This equation is able to handle both a Dirichlet and a Neumann boundary condition for the contact angles and needs to be studied more in the future.

2.2. Energy Dissipation of a Drop over a Time Interval. In this subsection, we derive the formula for the energy loss for the quasi-static process described by eq 6 and variational inequality 7 and describe the physical significance of the result.

Consider a liquid drop that evolves over $[t_0, t_f]$. During this time interval, energy dissipation of the drop is

$$\begin{aligned}\mathcal{E}(t_f, E(t_f)) - \mathcal{E}(t_0, E(t_0)) &= \int_{t_0}^{t_f}\left[\frac{d}{dt}\mathcal{E}(t, E(t))\right]dt \\ &= \int_{t_0}^{t_f}\left[\frac{d}{dt}\sigma_{LG}(|A_f(t)| - \cos\theta_Y|A_w(t)|)\right]dt \\ &\quad + \int_{t_0}^{t_f}\int_{\partial E(t)}\psi(x,t)\mathbf{v}\cdot\nu\,dS\,dt \\ &\quad + \int_{t_0}^{t_f}\int_{E(t)}\frac{\partial\psi(x,t)}{\partial t}\,dx\,dt\end{aligned}$$

Observe that

$$\begin{aligned}\int_{t_0}^{t_f}\int_{A_f(t)}(-2\sigma_{LG}H + \psi(x,t))v_f\,dS_f\,dt &= \int_{t_0}^{t_f}\int_{A_f}p(t)v_f\,dS_f\,dt \\ &= \int_{t_0}^{t_f}p(t)\frac{d}{dt}|E(t)|\,dt \\ &= \int_{t_0}^{t_f}p(t)\,\dot{\omega}(t)\,dt\end{aligned}$$

The above equations yield

DOI: 10.1021/la504495c
Langmuir XXXX, XXX, XXX−XXX

$$\mathcal{E}(t_f, E(t_f)) - \mathcal{E}(t_0, E(t_0)) = \int_{t_0}^{t_f} p(t)\,\dot{\omega}(t)\,dt + \int_{t_0}^{t_f}\int_{\Gamma} \sigma_{LG}(\cos\theta - \cos\theta_Y) v_c\,dl\,dt = \int_{t_0}^{t_f} p(t)\,\dot{\omega}(t)\,dt \quad (10)$$

due to flow rules (i)−(iii) arising from variational inequality 7, which dictate that for the advancing and receding angles, that is, when $\theta = \theta_A$ or $\theta = \theta_R$, we must have $\theta_Y = \theta$ if $v_c \neq 0$. For other angles $\theta \in (\theta_R, \theta_A)$, we must have $v_c = 0$.

Results from experiments described in section 3.1 reveal that the graph of the capillary pressure $p(t)$ versus the volume shows hysteresis (Figure 5a). Thus, we may describe the relation of p to ω by a rate-independent hysteresis operator,[13−16] that is,

$$p(t) = C_{r,s}[\omega; \psi_{-1}](t) \quad (11)$$

where C is a hysteresis operator and ψ_{-1} represents the initial configuration of the drop. The parameters of the hysteresis operator are $s = (\theta_A + \theta_R)/2$ and $r = (\theta_A - \theta_R)/2$.

The hysteresis operator is the result of the system defined by the nonlinear Young−Laplace equation (eq 6) with a Dirichlet boundary condition and variational inequality 7. This is similar to the hysteresis operator arising in plasticity (called the "stop operator" in the literature), which is due to a linear elastic element in combination with a variational inequality.[14] Other known basic hysteresis operators are the "play operator" and the "relay".[14]

We will show in section 3 that this new operator $C_{r,s}$ satisfies a property called "minor-loop closure" in a similar fashion to the stop, play, and relay operators. Just as the stop operator is a fundamental or basic unit from which more complex operators are defined, such as the Prandtl operator,[14] which is useful in describing plasticity, the play and relay operators are used to construct an operator called the Preisach operator that is used to describe scalar hysteresis in magnetism.[14] Operators $C_{r,s}$ may also be used to describe more complex drops that have varying Coulomb friction at the interface of the solid and liquid. We may define

$$p(t) = C[\omega; \psi_{-1}](t): = \int_0^{\infty}\int_0^{s} C_{r,s}[\omega; \psi_{-1}](t)\,\mu(r, s)\,dr\,ds \quad (12)$$

where μ is a non-negative weighting density function. C describes a general hysteresis operator that relates the capillary pressure p and the volume ω and needs to be studied further in the future.

2.2.1. Remarks. Alberti et al.[21] consider energy losses due to only line motion and do not consider the possibility that the capillary pressure might be related to the volume through a hysteresis operator. They introduce a kinetic friction-type functional on the right-hand side of eq 10 and obtain

$$\mathcal{E}(t_f, E(t_f)) - \mathcal{E}(t_0, E(t_0)) = \int_{t_0}^{t_f} p(t)\,\dot{\omega}(t)\,dt + k\int_{t_0}^{t_f}\int_{\Gamma} |v_c| dl\,dt$$

We may also introduce such a term and realize that the total losses have both a hysteresis component due to solid friction and a dynamic component due to kinetic friction. On the other hand, as a general hysteresis operator has an associated potential function $\mathcal{U}$ and a dissipation function $\mathcal{D}$ (ref 14), we have

$$p(t)\,\dot{\omega}(t) = \mathcal{U}[\omega; \psi_{-1}](t) + \left|\frac{d}{dt}\mathcal{D}[\omega; \psi_{-1}](t)\right| dt \quad (13)$$

Therefore,

$$\mathcal{E}(t_f, E(t_f)) - \mathcal{E}(t_0, E(t_0)) = \int_{t_0}^{t_f} \mathcal{U}[\omega; \psi_{-1}](t)\,dt + \int_{t_0}^{t_f}\left|\frac{d}{dt}\mathcal{D}[\omega; \psi_{-1}](t)\right| dt + k\int_{t_0}^{t_f}\int_{\Gamma} |v_c|\,dl\,dt \quad (14)$$

where the first term on the right-hand side represents the change in potential energy, the second term is the energy dissipated due to hysteresis, and the third term is the energy dissipated due to kinetic friction that opposes contact line motion. Figure 5 shows that when the magnitude of the volume change is small, there is no energy lost due to hysteresis, while there is no energy lost due to kinetic friction as there is no line motion. However, there is still some work done by the external agent that is changing the volume. Therefore, this work must go toward an increase or decrease in the potential energy of the system. The first term in eq 14 allows for this possibility.

3. DROPLET ON A PLATE: VALIDATION OF THEORY

In this section, we examine the effect of contact angle hysteresis caused by the adhesion between a liquid drop on a solid surface. We further calculate the dissipation of energy due to contact angle hysteresis. Before proceeding, we discuss how the contact angle is measured in experiments.

The contact angle is not simply the tangential angle at the point of contact.[9,10,30] In the region of the triple-point line (the line of contact between the substrate, gas, and liquid), the liquid exhibits three distinct regions: the molecular region, the transition region, and the capillary region for a liquid with a chemical affinity for a solid without total wetting taking place, such as a hydrophilic surface for water.[3] Within the molecular region, only a few molecules (on the order of 5 or 10) cover the surface;[10] therefore, interfacial tension overcomes the intraspecific molecular interactions, resulting in a concave shape.

In the transition region, the number of molecules increases to the point where intraspecific interactions begin to dominate. The result is a relatively straight surface in the transition region. In the capillary region, molecular interactions and liquid−gas surface tension dominate the relatively weak substrate−gas and liquid−gas interfacial tensions, forcing the surface into a convex shape. It is in the transition region where one should measure the angle of contact. The angle that the transition region makes with the substrate is the true contact angle to be used in the law of Young−Dupré.[9,10]

3.1. Results from Experiment and Numerical Simulations. In this subsection, we describe an experiment that demonstrates the hysteresis in contact angles caused by the adhesion between a liquid drop on a solid surface. Details of the experiment may be found in ref 31. Drops of distilled water were slowly added to a glass slide that had been cleaned with a nonpolar solvent. After each drop was stabilized on the slide, high-resolution images were taken of the top view and the side view of the drop with two cameras (Figure 3). After the diameter of the drop was observed to increase, we then

DOI: 10.1021/la504495c
Langmuir XXXX, XXX, XXX−XXX

removed liquid from the drop using a thin pipet and took more images of the top view and the side view.

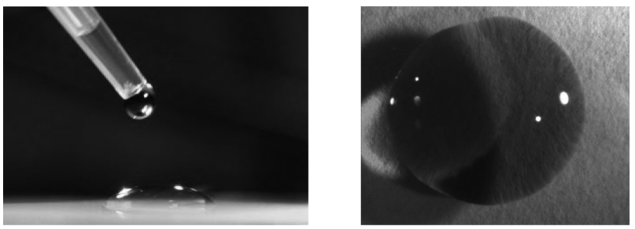

(a) (b)

Figure 3. (a) Side and (b) top views of the liquid droplet.

Contact angles were measured by analyzing the side-view images of the droplets as described in ref 31 using free open-source software program ImageJ. This software includes a function that performs angle measurements.[30,32] For each side-view image, we computed the contact angles on the left and right sides of the profile, and the results are shown in Figure 4. Clear evidence of contact angle hysteresis is observed with an approximate advancing angle at 45° and a receding angle at 12°. The rectangles drawn in Figure 4a,b show the extrapolated hysteresis effect.

The drops observed in the experiment were symmetric, that is, with a circular contact area between the glass slide and the water and equal contact angles along the contact line. For a symmetric drop, the Young–Laplace equation (eq 6) simplifies to[31]

$$\left(\left(\frac{xh'}{\sqrt{1+h'^2}}\right)' + \frac{(p-\rho g h(x))x}{\gamma_{LG}}\right) = 0 \;\forall\; x \in [0, R] \tag{15}$$

where x denotes the radial distance from the center of the drop, $h(x)$ describes the height of the drop at x, $h(0)$ is the height of the drop in the center, and $h(R)$ is zero. p is the capillary pressure.

On the basis of the top view of the droplets (Figure 3b), we measure the droplet radius that corresponds to each measured contact angle. The meniscus profile, eq 15, is solved to find the capillary pressure p values for which we have $h(R) = 0$ and $h'(0) = 0$. Here, R is the value observed in the experiments, and the two-point boundary value problem is solved using the modified simple-shooting method described in ref 33. Once the height of the drop is solved for, the corresponding volume can be found easily: volume $= \int_0^R 2\pi x\, h(x)\, dx$. The results are tabulated in Table 1. The capillary pressure and volume are computed for the measured angles and diameters and plotted in Figure 5a using asterisks.

Table 1. Droplet Diameter and Contact Angle Measurements and the Corresponding Capillary Pressure and the Droplet Volumes[a]

d(mm)	θ(deg)	p(N/m^2)	volume × 10^{-7} (m^3)
15.0	43.72	25.02	2.063
16.5	45.48	25.34	2.757
18.0	45.61	24.93	3.452
22.9	46.26	24.32	6.261
25.4	45.50	23.64	7.908
25.4	40.29	21.00	6.957
25.6	36.97	19.29	6.514
25.4	36.26	18.44	6.059
25.4	28.25	14.84	4.830
25.1	19.14	10.12	3.182
22.9	12.43	6.68	1.638
16.8	12.59	7.21	0.765

[a]The capillary pressure and droplet volume were computed by solving eq 15 with a Dirichlet boundary condition and data from experiment. Other parameters used in the computation are the surface tension of water γ_{LG} = 0.073J/m^2, the density of water ρ = 1000 kg/m^3, and the acceleration due to gravity g = 9.81 m/s^2.

Next, we perform a numerical experiment where the Young–Laplace equation (eq 6) with the variational inequality (7) and a Dirichlet boundary condition are solved with the volume prescribed as a function of time. The system is solved using COMSOL software for each instant in time, with the contact angles computed at each step serving as initial conditions for the next. The results are plotted in Figure 5a with a solid blue line. The match between the data from experiment and those predicted by theory may be noted.

We continue our study of the Young–Laplace equation (eq 6) with the variational inequality (7) by studying the capillary

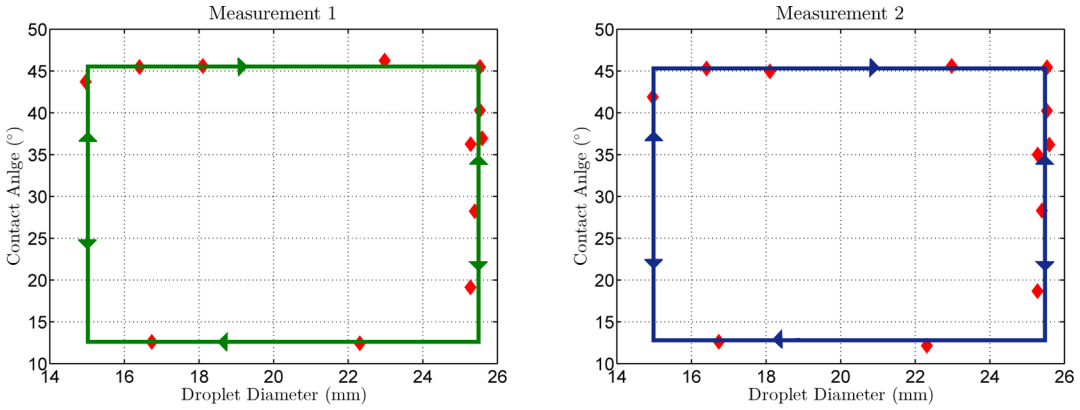

(a) (b)

Figure 4. Contact angle hysteresis diagrams for measurements 1 and 2. Contact angles versus droplet diameter for volume addition and subtraction of the liquid drop on the substrate.

DOI: 10.1021/la504495c
Langmuir XXXX, XXX, XXX–XXX

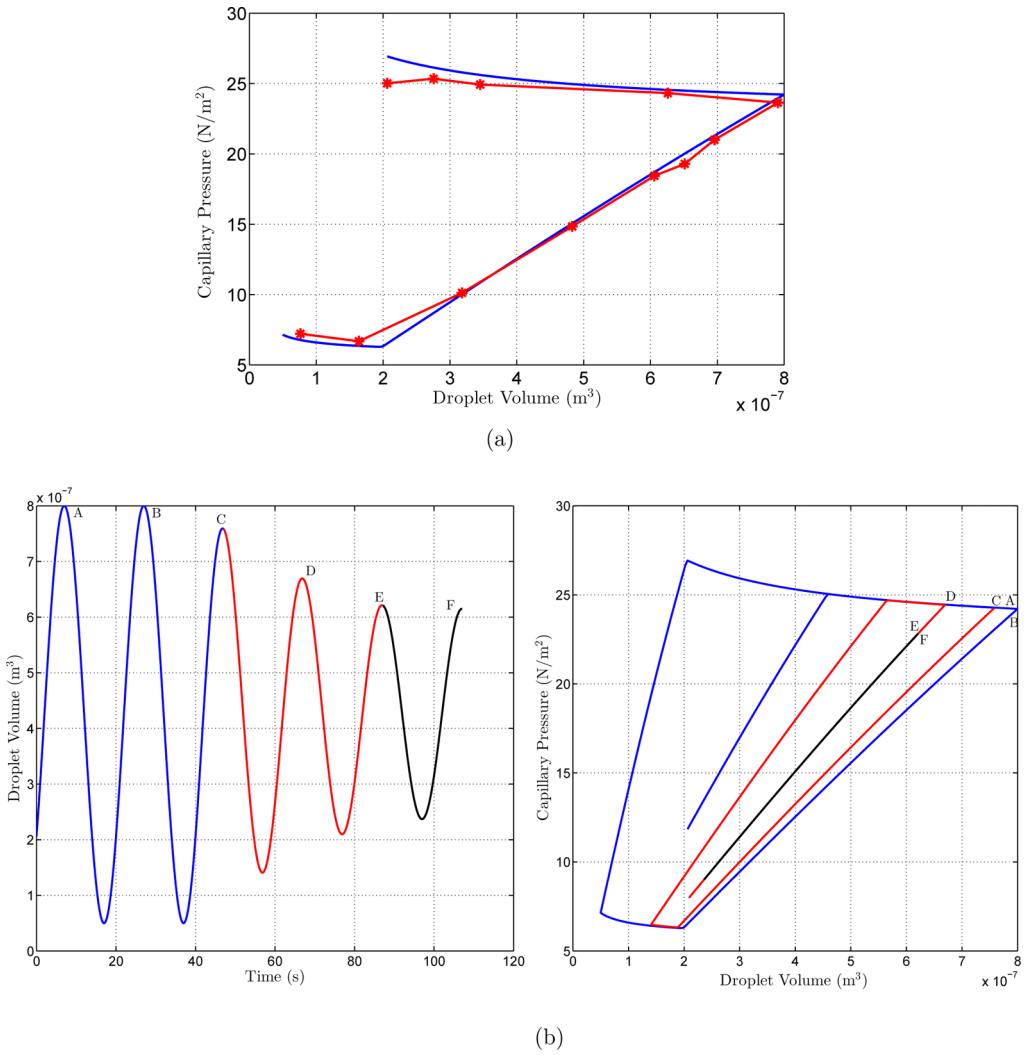

Figure 5. (a) Capillary pressure and volume are computed for the measured angles and diameters in Table 1 and plotted with asterisks. The computation is based on the solution of a two-point boundary value problem using measured diameters and contact angles. The solid blue line is the result of solving the Young−Laplace equation (eq 6) with a Dirichlet boundary condition and the variational inequality (7) using COMSOL software. Here, the volume variation is prescribed as a function of time. (b) The panel on the left shows the prescribed variation of volume with time. The panel on the right shows that minor loops close on each other just as in magnetism or plasticity.

pressure versus volume relation for a more complex volume variation as shown in Figure 5b. The parameters used in this simulation study are the same as those used in Figure 5a. The peaks in the volume variation are marked with letters A−F. It may be noted that as the volume changes from A to B or E to F, the capillary pressure versus volume relation shows a closed graph (blue and black solid lines). Furthermore, the solid red line exhibits behavior that is very much like what is observed in magnetism or plasticity. As the volume traces a path from C to D, the capillary pressure versus volume graph attempts to close the loop but is unable to do so as the volume starts decreasing from D.

4. CONCLUSIONS

The main contribution of this article is the finding that capillary pressure versus volume for a liquid drop on a solid is hysteretic and shows the same properties as the well-known hysteresis operators used to describe plasticity and magnetism. We also showed that the capillary pressure versus volume relation may be derived using the calculus of variations by minimizing the Helmholtz free energy subject to the condition that the surface energy of the contact area between the solid and liquid takes values in a closed and bounded interval. Although the capillary effect phenomenon is complex and the contact line where the solid−liquid−gas phases meet may be pinned at different places, the capillary pressure is a single scalar variable that is constant throughout the liquid for a given volume and encapsulates the distributed contact angle information along the contact line. The graph of capillary pressure versus volume shows hysteresis, and a simple area calculation immediately yields the energy loss due to overcoming the Coulomb friction at the solid−liquid interface.

AUTHOR INFORMATION

Corresponding Author

*E-mail: bhagya.athukorala@ttu.edu.

Notes

The authors declare no competing financial interest.

DOI: 10.1021/la504495c
Langmuir XXXX, XXX, XXX−XXX

REFERENCES

(1) de Gennes, P. G.; Brochard-Wyart, F.; Quéré, D. *Capillarity and Wetting Phenomena: Drops, Bubbles, Pearls, Waves*; Springer: New York, 2003.

(2) Sulman, H. L.; Picard, H. K. *The Theory of Concentration Processes Involving Surface-Tension*; Columbia University, New York, 1920; original typewritten notes.

(3) de Gennes, P. G. Wetting: Statics and Dynamics. *Rev. Mod. Phys.* **1985**, *57*, 828−861.

(4) Dettre, R.; Johnson, R., Jr. In *Contact Angle, Wettability, and Adhesion*; Fowkes, F., Ed.; American Chemical Society: Washington, DC, 1964; pp 136−144.

(5) Penn, L.; Miller, B. A study of the primary cause of contact angle hysteresis on some polymeric solids. *J. Colloid Interface Sci.* **1980**, *1*, 238−241.

(6) Ramos, S.; Charlaix, E.; Benyagoub, A. Contact angle hysteresis on nano-structured surfaces. *Surf. Sci.* **2003**, *540*, 355−362.

(7) Chibowski, E.; Malgorzata, J. Comparison of contact angle hysteresis of different probe liquids on the same solid surface. *Colloid Polym. Sci.* **2013**, *291*, 391−399.

(8) Marmur, A. In *Contact Angle, Wettability, and Adhesion*; Mittal, K. L., Ed.; VSP: Boston, 2009; pp 3−18.

(9) Merchant, G. J.; Keller, J. B. Contact Angles. *Phys. Fluids A* **1992**, *4*, 477−485.

(10) Snoeijer, J.; Andreotti, B. A microscopic view on contact angles. *Phys. Fluids* **2008**, *20*, 057101.

(11) Extrand, C. W. A thermodynamic model for contact angle hysteresis. *J. Colloid Interface Sci.* **1998**, *207*, 11−19.

(12) Athukorallage, B.; Iyer, R. Model of a Contact Lens and Tear Layer at Static Equilibrium. *Proc. Am. Control Conf.* **2013**, 3605−3612.

(13) Krasnosel'skii, M. A.; Pokrovskii, A. V. *Systems with Hysteresis*; Springer-Verlag: Berlin, 1989.

(14) Brokate, M.; Sprekels, J. *Hysteresis and Phase Transitions*; Springer-Verlag: New York, 1996.

(15) Visintin, A. *Differential Models of Hysteresis*; Springer: Berlin, 1994.

(16) Krejč, P. *Hysteresis, Convexity and Dissipation in Hyperbolic Equations*; GAKUTO International Series; Gattötoscho, 1996.

(17) Santos, M.; White, J. Theory and Simulation of Angular Hysteresis on Planar Surfaces. *Langmuir* **2011**, *27*, 14868−14875.

(18) Santos, M.; Velasco, S.; White, J. Simulation Analysis of Contact Angles and Retention Forces of Liquid Drops on Inclined Surfaces. *Langmuir* **2012**, *28*, 11819−11826.

(19) Janardan, N.; Panchagnula, M. V. Effect of the Initial Conditions on the Onset of Motion in Sessile Drops on Tilted Plates. *Colloids Surf., A* **2014**, *456*, 238−245.

(20) Chen, H.; Amirfazli, A.; Tang, T. Modeling Liquid Bridge between Surfaces with Contact Angle Hysteresis. *Langmuir* **2013**, *29*, 3310−3319.

(21) Alberti, G.; DeSimone, A. Quasistatic Evolution of Sessile Drops and Contact Angle Hysteresis. *Arch. Ration. Mech. Anal.* **2011**, *202*, 295−348.

(22) Johnson Jr., R.; Dettre, R. In *Contact Angle, Wettability, and Adhesion*; Fowkes, F., Ed.; American Chemical Society: Washington, DC, 1964; pp 112−135.

(23) Alberti, G.; DeSimone, A. Wetting of rough surfaces: a homogenization approach. *Proc. R. Soc. A* **2005**, *461*, 79−97.

(24) Turco, A.; F, A.; DeSimone, A. Wetting on rough surfaces and contact angle hysteresis: Numerical experiments based on a phase field model. *ESAIM: Math. Modell. Numer. Anal.* **2009**, *43*, 1027−1044.

(25) Fideli, L. Numerical Techniques for the Study of Wetting on Rough Surfaces and Contact Angle Hysteresis. Ph.D. Thesis, Scuola Internazionale Superiore di Studi Avanzati, Trieste, Italy, 2011.

(26) Cacace, S.; Chambolle, A.; DeSimone, A.; Fedeli, L. Macroscopic contact angle and liquid drops on rough solid surfaces via homogenization and numerical simulations. *ESAIM: Math. Modell. Numer. Anal.* **2013**, *47*, 837−858.

(27) Stowe, K. *An Introduction to Thermodynamics and Statistical Mechanics*; Cambridge University Press, 2007.

(28) Luenberger, D. *Optimization by Vector Space Methods; Professional Series*; Wiley, 1968.

(29) Zhong-can, O.; Helfrich, W. Bending Energy of Vesicle Membranes: General expressions for the first, second, and third variation of the shape energy and applications to spheres and cylinders. *Phys. Rev. A* **1989**, *39*, 5280−5288.

(30) Lin, S.-Y.; Chang, H.-C.; Lin, L.-W.; Huang, P.-Y. Measurement of Dynamic/Advancing/Receding Contact Angle by Video-Enhanced Sessile Drop Tensiometry. *Rev. Sci. Instrum.* **1996**, *67*, 2852−2858.

(31) Athukorallage, B. Capillarity and Elastic Membrane Theory from an Energy Point of View. Ph.D. Thesis, Texas Tech University, 2014.

(32) Broesch, D. J.; Dutka, F.; Frechette, J. Curvature of Capillary Bridges as a Competition Between Wetting and Confinement. *Langmuir* **2013**, *29*, 15558−15564.

(33) Holsapple, R. W.; Venkataraman, R.; Doman, D. New, Fast Numerical Method for Solving Two-Point Boundary-Value Problems. *J. Guid., Control, Dyn.* **2004**, *27*, 301−304.

DOI: 10.1021/la504495c
Langmuir XXXX, XXX, XXX−XXX